Swell-shrink and hydraulic behaviour of compacted red soil-bentonite mixture

Swell-shrink and hydraulic behaviour of compacted red soil-bentonite mixture

Devapriya A S and Thyagaraj T

Department of Civil Engineering, Indian Institute of Technology Madras, Chennai 600036, India

devapriya.as09@gmail.com

Abstract. Clay liners are provided in waste landfills to prevent the leachate from percolating into underlying soil and ground water and polluting it. Hence, soils used as landfill liners must possess low hydraulic conductivity (< 10^{-7} cm/s). In the initial as-compacted state, liners satisfy this design criterion. However, in the field, liners are subjected to alternate wet-dry cycles and the initial microstructure of liners change, thereby affecting their hydraulic properties. The present study was conducted on a locally available red soil mixed with bentonite so that it satisfies the requirement of hydraulic conductivity in the as-compacted state. To achieve this objective, identical specimens compacted at optimum moisture content to its maximum dry density were inundated with distilled water under a surcharge load of 12.5 kPa. Upon attainment of maximum swelling, hydraulic conductivity tests were conducted at swollen state under a hydraulic gradient of 20. The soil specimens were then dried at a temperature of 45±2 °C. The weight, height and diameter of specimens were measured continuously during drying to study the shrinkage behaviour of the soil. The dried specimens were subjected to subsequent wet-dry cycles until the specimens reached an equilibrium state and the hydraulic conductivity was determined after each wetting cycle. SEM images were also captured to analyse the changes in the soil structure in the as-compacted state and at the end of different wetting cycles.

1. Introduction

Compacted clay liners are provided in both hazardous and municipal waste landfills to prevent the leachate from percolating into the underlying soil and polluting the soil and ground water [1]. Soils in arid and semi-arid region undergo seasonal moisture fluctuations throughout the year [2]. This variation in the moisture subjects the compacted clay liner to alternate wet-dry cycles resulting in periodic swelling and shrinkage of the soil [3]. For compacted clay liners to be effective as barriers, they must possess a very low hydraulic conductivity. Generally, the design of compacted liners is based on the assumption that the soils having a laboratory measured hydraulic conductivity of 1×10^{-7} cm/s will have little leakage in the field. However, the performance evaluation of compacted clay liners has shown a higher hydraulic conductivity value [4]. In the field, as the clay liners are subjected to seasonal moisture fluctuations, evapotranspiration, groundwater fluctuations and heat generated from landfill, they are subjected to alternate swell-shrink movements and desiccation cracking that changes the as-compacted nature of the liner [5]. The cracks formed during a drying cycle may not fully heal during the subsequent

wetting cycle, and hence they end up being planes of weakness in soil and act as preferential flow paths for the leachate. This results in the increased hydraulic conductivity [6].

The swell potential of soil increases with the number of wet-dry cycles when the soil is completely dried to a water content less than its shrinkage limit. The increase in swell potential continues till the soil reaches an equilibrium state, when the vertical deformations become constant. The equilibrium bandwidth and equilibrium cycle depend on the composition of the soil, clay mineralogy and the type of contact between particles. Previous studies have reported that most of the soils reach the equilibrium cycle in 3 to 5 cycles. Maximum shrinkage occurs during the first drying cycle, after which it gradually reduces till it reaches equilibrium [7].

Alternate wetting and drying of soils cause destruction of contacts in soils gradually. With the number of wet-dry cycles, the large aggregates break off and disorientation of structural elements occur [8]. Compacted soil in its as-compacted state is characterized with bimodal pore size distribution consisting of macrovoids and microvoids. When soil is saturated, microvoids expand and fill into macrovoids changing the bimodal distribution to unimodal [9].

Even though extensive research is carried out on the behaviour of compacted clay during wet-dry cycles, the studies bringing out the effect of wet-dry cycles on red soil-bentonite mixtures are not available. Therefore, the present study focuses on bringing out the effect of wet-dry cycles on the swell-shrink behaviour of compacted red soil-bentonite mixture. To achieve this objective, a locally available red soil was collected and used for the present study. The locally available red soil met all the EPA requirements and satisfies all the design criteria except the hydraulic conductivity criterion, which was overcome by addition of 20% bentonite to red soil. The red soil-20% bentonite mixture meets the hydraulic conductivity criterion of 10^{-7} cm/s in its as compacted state. Further, the red soil-bentonite mixture was subjected to wet-dry cycles to simulate the field seasonal moisture variations. Scanning Electron Microscopy (SEM) studies were also carried out for understanding the swell-shrink and hydraulic behaviour.

2. Soils used for the study

The current study is carried out on red soil sourced from IIT Madras campus, Chennai, India and sodium bentonite. The red soil was air-dried, pulverized and sieved through No. 10 sieve. Dry bentonite was added to account for 20% by dry weight of the red soil. The characteristics of red soil, bentonite and the red soil-bentonite mixture are presented in table 1.

3. Experimental programme

3.1. Preparation of soil specimen

To the dry red soil-bentonite mixture, the required volume of distilled water was added to attain the moisture content corresponding to the optimum moisture content of the red soil-20% bentonite mixture. This red soil-bentonite mixture was kept in sealed polythene cover and was stored in the desiccator for 48 h for moisture equilibration. After 48 h, the moisture content of the soil was measured to ensure that the target moisture content has been achieved. Identical specimens were then prepared by statically compacting the pre-wetted soil mixture in stainless steel rings of 75 mm diameter and 30 mm height, to a thickness of 20 mm so that its standard Proctor maximum dry density was attained.

3.2. Oedometric swell-shrink tests

Identical test specimens were prepared and kept between two dry porous stones and filter papers, and the oedometric rings were secured in its position in the oedometric cell. The free movement of top porous stone was ensured so that vertical swelling occurs without any hindrance. The oedometer cells were placed in the test set-up and a surcharge load of 12.5 kPa was applied. The specimens were then inundated with distilled water. Vertical movements were noted using a dial gauge of 0.002 mm least count, until the readings became constant. The percentage swell was calculated using equation 1.

$$Swell\ (\%) = \frac{\Delta H}{H} \times 100 \quad (1)$$

Where ΔH is the increase in height of soil specimen during swelling and H is the initial as-compacted height of soil specimen for the first wetting cycle and the shrunken height of the specimen for the subsequent wetting cycles.

Table 1. Characteristics of soils used in the study.

Property	Red soil	Bentonite	Red soil + 20% bentonite
Specific gravity	2.68	2.92	2.73
Sand (%)	66	0	55
Silt (%)	15	29	16
Clay (%)	19	71	29
Liquid limit (%)	34	224	113
Plastic limit (%)	20	48	35
Shrinkage limit (%)	15	8.4	13
Plasticity index (%)	14	176	78
Soil classification	SC	CH	SC
Standard Proctor maximum dry density (Mg/m^3)	1.98	-	1.79
Optimum moisture content, OMC (%)	11	-	15
Unconfined compressive strength[a] (kPa)	212	-	251

[a] Specimen compacted to standard Proctor maximum dry density at OMC.

After complete swelling of the specimen, water was removed from the oedometric cell, the load was also removed and then the test set-up was dismantled. Firstly, the weight and height of the specimen were measured to calculate the water content, the degree of saturation and the volume of the specimen. Then, the soil specimens were allowed to completely dry at a temperature of 45 ± 2 ℃ under the same vertical load of 12.5 kPa. During drying, the height and diameter of the specimen were measured continuously using height gauge and vernier callipers, respectively, and the weight was also noted, until the vertical and volumetric deformations became constant. These readings were used to calculate the volume change, void ratio and water content at intermediate stages of drying of the specimen. The drying was accelerated by allowing the specimen to dry at a temperature of 45±2 ℃. The void ratio of the specimens can be calculated using equations 2 and 3.

$$\rho_d = \frac{\rho}{1+w} \quad (2)$$

$$\rho_d = \frac{G_s \rho_w}{1+e} \quad (3)$$

The degree of saturation can be calculated using the equation 4.

$$eS_r = wG_s \quad (4)$$

Where, ρ_d is the dry density, ρ is the bulk density, w is the water content, G_s is the specific gravity of the soil, ρ_w is the density of water, e is the void ratio and S_r is the degree of saturation.

As the soil specimen dried, shrinkage occurred in both vertical and lateral directions. In order to carry out the next cycle of wetting, the completely dried soil specimen was placed centrally in the oedometric ring and the test setup was assembled as explained above. The soil specimen was then again inundated with distilled water and the procedure of wetting and drying was repeated until the soil specimen

completed 5 alternate wet-dry cycles. At the 5th wet-dry cycle, the soil specimen reached the equilibrium, wherein the swell-shrink movements of subsequent cycle became constant.

3.3. Hydraulic conductivity tests

After each wetting cycle when the soil attains equilibrium swelling, the hydraulic conductivity was measured on the swollen soil specimens using the falling head method in rigid wall permeability test set-ups conforming to ASTMD 5856-15 [9]. The specimens were subjected to the same surcharge load of 12.5 kPa and a hydraulic gradient of 20.

3.4. Scanning Electron Microscopic studies

Scanning Electron Microscopy (SEM) was performed on identical red soil-bentonite specimens in the as-compacted state and after different wetting cycles using a Quanta FEG 200 high-resolution scanning electron microscope. For SEM studies, undisturbed soil samples of 1 cm^3 were extruded by statically pushing a thin tube into the compacted red soil-bentonite specimens. The samples were freeze-dried to preserve the soil structure and were then gold coated at high vacuum using a sputtering machine. The gold coated samples were then mounted on aluminium mounting disks and the SEM imaging was performed.

4. Results and discussion

4.1. Effect of wet-dry cycles on swell potential

Figure 1 shows the variation of swell potential with wetting cycles of compacted red soil-bentonite specimen. It can be observed from the figure that the swell potential increased with the wetting cycles till the 3rd wetting cycle, after which the swell potential decreased. It is clear that the 5th wetting cycle is the equilibrium cycle where the swell becomes equal to the swell attained during the previous cycle. As the soil specimens were inundated with distilled water, the specimens absorbed water into the void spaces for dissipation of matric suction. The as-compacted soil specimen which is characterized with a higher water content has the least matric suction compared to dried specimens at the end of drying cycles. Hence the swell potential is more during the subsequent wetting cycles [10]. The swell potential reduces after the 3rd wetting cycle owing to fatigue by swelling [11].

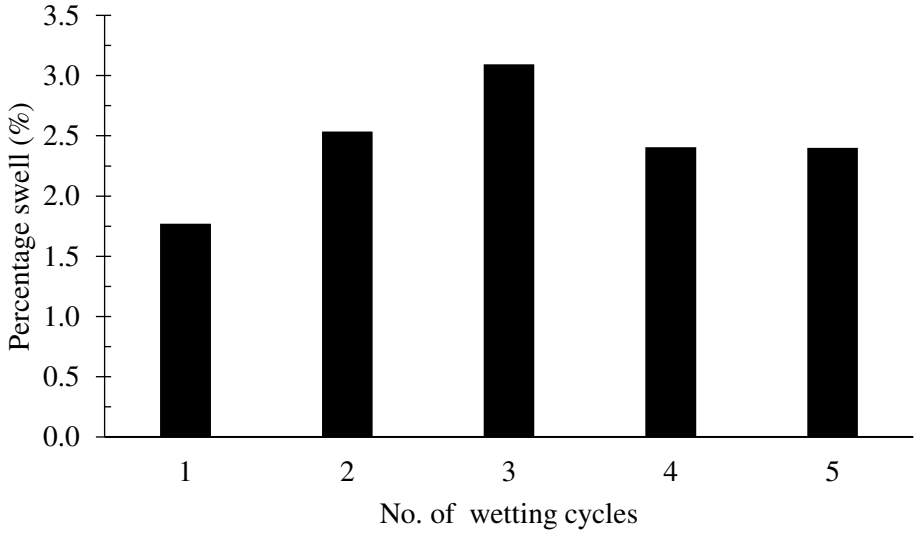

Figure 1. Percentage swell of red soil-bentonite mixture with wetting cycles.

4.2. Shrinkage and e-w plots

The variation of void ratio with water content (e-w plots) of the drying paths were plotted during each drying cycle. The plots being similar only the 1st, 3rd and 5th drying cycles are presented in figure 2. The e-w plots are S-shaped which distinctly show the three different stages of shrinkage– structural shrinkage, normal shrinkage and residual shrinkage. As the soil specimens attained 100% saturation during wetting cycles, the plots start from the 100% saturation line and gradually move away from it as the soil specimens dry and become unsaturated. Initially, during the structural shrinkage, water is lost from larger pores in the soil and the reduction of void ratio is very less compared to the loss of water content. The void ratio at the beginning of 3rd drying is higher than other cycles, owing to the larger percentage of swell occurred during the 3rd wetting cycle. The void ratio at full saturation decreases in the subsequent cycles, but it is always greater than the void ratio attained after the first wetting cycle. As the soil specimens reach the stage of normal shrinkage, there is a rapid reduction in the volume of soil with the reduction in the water content. At this stage of drying, the e-w plots take a 45° slope, till the water content of the specimens approach the shrinkage limit. As the soil reaches the stage of residual shrinkage, the reduction in the volume of soil is reduced with the reduction in the water content [12].

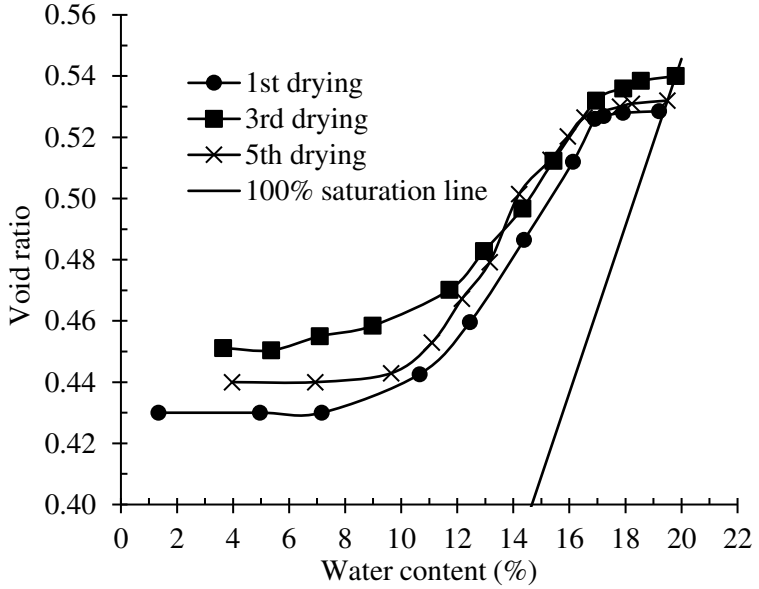

Figure 2. Void ratio-water content (e-w) plots during 1st, 3rd and 5th drying.

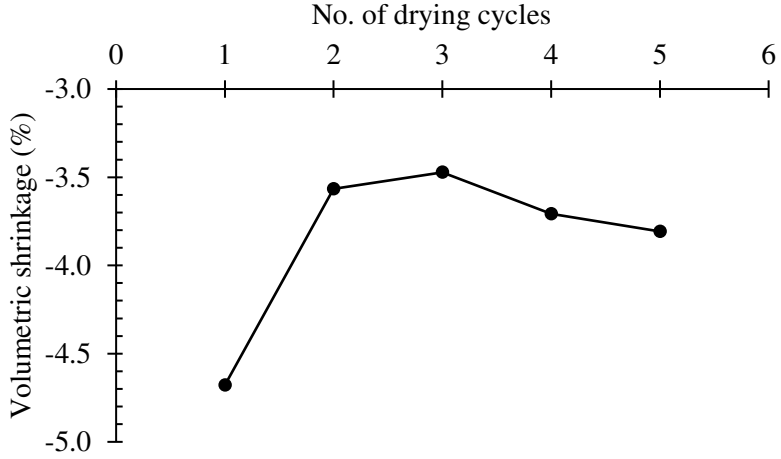

Figure 3. Variation of volumetric shrinkage with drying cycles.

Further, the void ratio and water content at the end of 1st drying cycle is the lowest, which then increased with the subsequent wet-dry cycles. This indicates the soil density decreases as the soil specimens are subjected to wet-dry cycles.

Figure 3 plots the variation of volumetric shrinkage with drying cycles. It is clear that the volumetric shrinkage was maximum during the first drying and it further reduced with the number of wet-dry cycles. From figures 2 and 3, it can be noted that as the compacted soil specimen is subjected to alternate wet-dry cycles, the overall volume of the soil specimen increased, which indicates an expansion of soil aggregate.

4.3. Hydraulic conductivity

During drying, the microcracks were developed in the soil specimen, which acted as preferential flow paths. During subsequent rehydration, the soil expands, closing these microcracks. Figure 4 shows that the hydraulic conductivity slightly decreased up to the 3rd cycle and then slightly increased with the subsequent wet-dry cycles, which suggests that not all cracks were healed after complete swelling of soil. Further, it can be seen that the hydraulic conductivity is consistent with the swell plots, with hydraulic conductivity value being least for the 3rd wetting cycle. The swelling was maximum during the 3rd wetting cycle which resulted in maximum expansion of soil aggregate and hence the closure of most of the shrinkage cracks and intervoids during the 3rd wetting cycle. It should be noted here that even with multiple wet-dry cycles, the hydraulic conductivity values were always within the acceptable range.

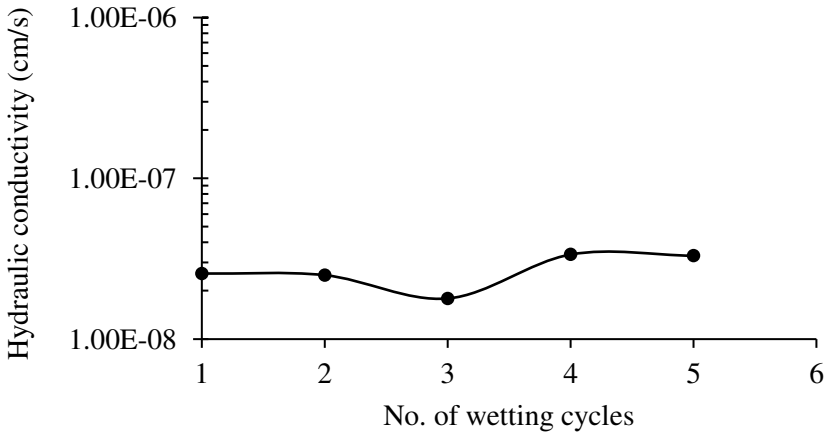

Figure 4. Variation of hydraulic conductivity with wetting cycles.

4.4. Microstructure

The change in the soil structure due to alternate wet-dry cycles is analysed using the Scanning Electron Microscopy (SEM) on identical soil specimens prepared at different conditions of the compacted red soil-20% bentonite mixture. The initial double structure of the soil consisting of macrovoids (inter-aggregate voids) and microvoids (intra-aggregate) is clearly visible in the SEM micrograph of the as-compacted state (figure 5a). Figure 5b shows that after first wetting, the macro-voids in the red soil-bentonite mixture disappeared, as the red soil-bentonite mixture swelled, expanding the microvoids. Further wetting of the soil makes the soil fabric more uniform with further reduction in the macrovoids (figure 5c). It should be noted here that all the shrinkage cracks were not closed even after full swelling (figure 5d).

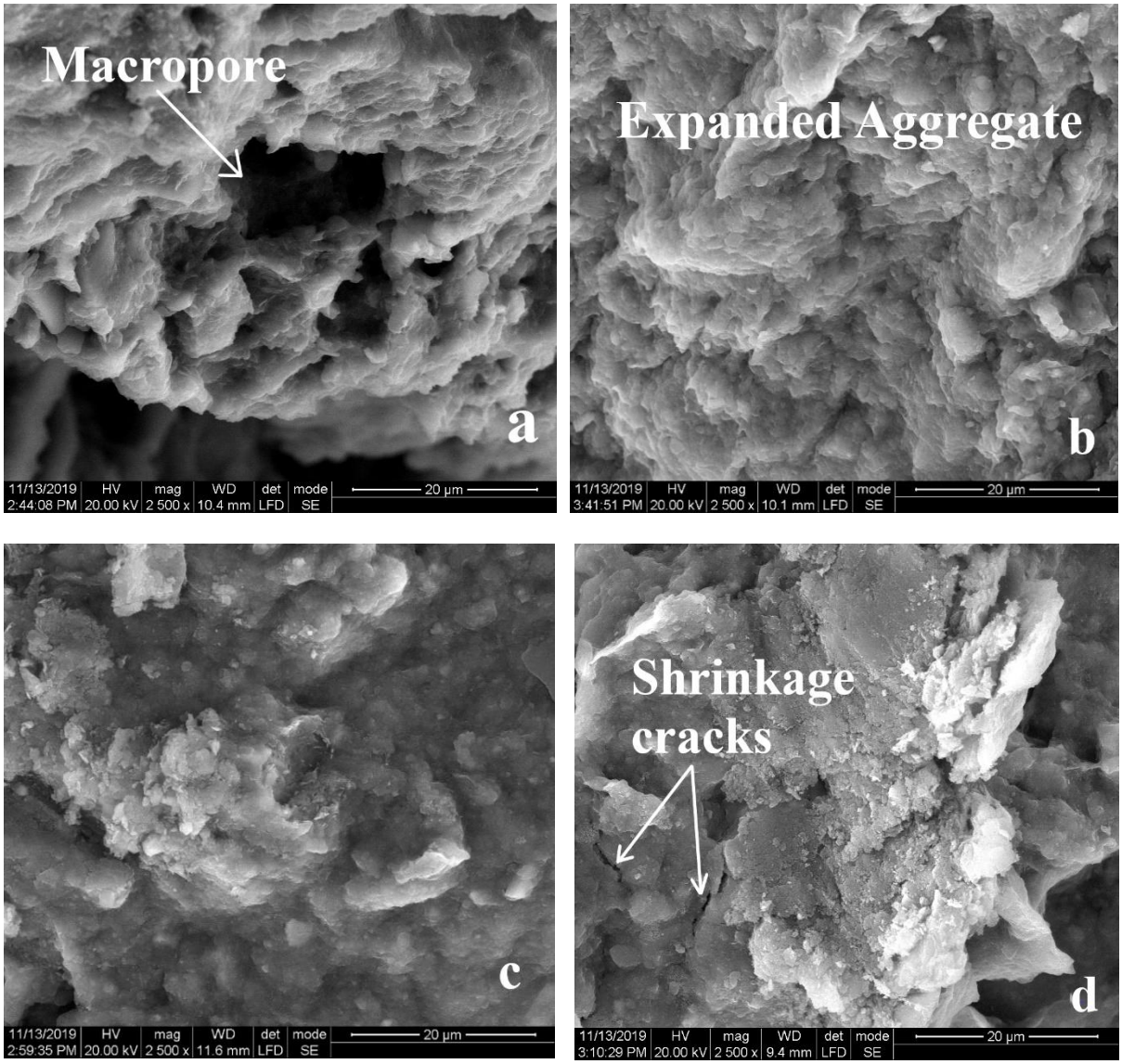

Figure 5. SEM micrographs of compacted red soil-bentonite mixture: a) in as-compacted state b) after 1st wetting cycle c) after 3rd wetting cycle and d) after 5th wetting cycle.

5. Conclusions

The present study investigated the swell-shrink and hydraulic behaviour of compacted red soil-bentonite mixture. The following conclusions were drawn from the present study:

- The swell potential of compacted red-soil bentonite mixture increased with the number of wet-dry cycles and the maximum swell was observed at the 3rd wetting cycle. The soil reached the equilibrium state at the 5th wetting cycle when the vertical and volumetric deformations become constant.
- The volumetric shrinkage of the compacted specimen was observed to be maximum during the first drying cycle, and after which it reduced.
- With the progression of wet-dry cycles, the large soil aggregates were destroyed with the disorientation of structural elements. As the soil specimen reach the equilibrium wetting cycle, the SEM images show a uniform dispersed structure with no macropore and homogenous micropore space.

- The hydraulic conductivity of compacted soil increased only slightly with the number of cycles, and always remained within the acceptable range.

Thus, the study shows that red soil-bentonite mixture could be a suitable material for constructing compacted clay liners and covers in landfills. The results presented in this paper are preliminary and necessitates an extensive research to bring out further behavioural characteristics of red soil-bentonite mixtures when subjected to alternate wet-dry cycles.

6. References

[1] Daniel D E and Benson C H 1990 *J. Geotech. Engrg.* **116** 1811
Benson C H and Trast J M 1995 *Clays and Clay Minerals* **43** 669-81
McBrayer M C, Mauldon M, Drumm E C and Wilson G V 1997 *J. Geotech. Geoenviron. Engg.* **123** 469-73
[2] Daniel D E and Wu Y-K 1993 *J. Geotech. Engrg.* **119** 223-37
Rao K S S, Sudhakar M and Gangadhara S 2000 *Geotech. Testing J.* **23** 193-98
[3] Dif A E, Bluemel W F 1991 *Geotech. Testing J.* **14** 96-102
Basma A A, Al-Homoud A S , Malkawi A I H, Al-Bashabsheh M A 1996 *Applied Clay science* **11** 211-27
[4] Omidi G H, Thomas J C, Brown K W 1996 *Water, Air and Soil Pollution* **89** 91-103
US EPA 2009 *Industrial Waste Management: Protecting Land, Ground Water, Surface Water, and Air* chapter 7, 7B-1-30
[5] Khire M V, Benson C H and Bosscher P J 1997 *J. Geotech. Geoenviron. Engg.* **123** 744-54
[6] Omidi G H, Thomas J C, Brown K W 1996 *Water, Air and Soil Pollution* **89** 91-103
Albrecht B A and Benson C H 2001 *J. Geotech. Geoenviron. Engg* **127** 67-75
[7] Basma A A, Al-Homoud A S , Malkawi A I H, Al-Bashabsheh M A 1996 *Applied Clay science* **11** 211-27
Tripathy S, Rao K S S, Fredlund D G 2002 *Can. Geotech. J.* **39** 938-59
[8] Basma A A, Al-Homoud A S, Malkawi A I H, Al-Bashabsheh M A 1996 *Applied Clay science* **11** 211-27
Osipov V I, Bik N N, Rumjantseva N A 1987 *Applied Clay science* **2** 363-74
[9] ASTM D5856-15 2015 *Standard test method for measurement of hydraulic conductivity of porous material using a rigid-wall, compaction-mold permeameter* ASTM Int'l (West Conshohocken, PA, US)
[10] Gens A and Alonso E E 1992 *Can. Geotech. J.* **29** 1013-32
[11] Tripathy S, Rao K S S 2009 *Geotech. Geol. Engg.* **27** 89-103
[12] Tripathy S, Rao K S S, Fredlund D G 2002 *Can. Geotech. J.* **39** 938-59
T Thyagaraj, Thomas S R, Das A M 2017 *Int. J. Geomech.* **17(2)** 06016013